Electronic Supplementary Material (ESI) for ChemComm.

Supporting Information

Mechanistic Insight into CdSe Nanoplatelet-Sensitized Upconversion: Size and Stacking Induced Effects

Zachary A. VanOrman,[1] Rachel Weiss,[1] Alexander S. Bieber,[1] Banghao Chen,[1] and Lea Nienhaus[1,]*

[1]Department of Chemistry and Biochemistry, Florida State University, Tallahassee, FL 32306, USA

*corresponding Author: lnienhaus@fsu.edu

Materials

Sodium myristate, cadmium nitrate tetrahydrate, methanol, octadecene, selenium, cadmium acetate dihydrate, oleic acid, ethanol, hexanes, chlorobenzene, rubrene, and toluene were purchased from Millipore Sigma. 9,10-Anthracenecarboxylic acid (ACA) and 9,10-diphenylanthracene (DPA) were purchased from TCI Chemicals. All reagents were used as received without purification excepting cadmium acetate dihydrate, oleic acid, and octadecene, which were degassed at 100 °C for ~6 h before being stored in an N_2-filled glovebox.

Cadmium Myristate Synthesis

Cadmium myristate ($Cd(myr)_2$) was synthesized according to Bertrand *et al.*[1] Briefly, 5 g of sodium myristate and 3 g of cadmium nitrate tetrahydrate were dissolved in 250 mL and 500 mL of methanol, respectively. After dissolution, the cadmium nitrate solution was added dropwise to the sodium myristate solution. After 2 hours of stirring, the white precipitate was filtered and washed thrice with methanol. The synthesized $Cd(myr)_2$ was then vacuum dried before transferring to a N_2 glovebox.

5.5 ML CdSe NPL Synthesis

5.5 monolayer CdSe NPLs were synthesized according to Ithurria *et al.,*[2] with modifications. 400 mg of $Cd(myr)_2$ and 30 mL of octadecene (ODE) were added into a 3-neck flask and degassed at 120°C for 1 hr. The temperature was then increased to 250°C, where 40 mg of Se in 2 mL of ODE were quickly injected. After the solution turned orange (~30 seconds), 395 mg of dried cadmium acetate was injected. 5 mL aliquots were taken out of the flask every 5 minutes, where 1 mL of oleic acid was added to each aliquot. The aliquot solutions were then transferred into a glovebox with a N_2 atmosphere, where they were purified by adding 5 mL of ethanol followed by centrifugation at 6000 rpm for 15 min. Each aliquot was redispersed in 1 mL of hexanes, and then syringe filtered using a 0.45 μm syringe filter.

NPL/ACA Ligand Exchange Procedure

Stock solutions of the NPL solutions were made so that the final UC solution would feature NPLs at a concentration of 1.07 X 10^{-7} M based on their calculated absorption coefficients (see Supporting Information for more detail on absorption coefficients).[3] Solutions of NPLs and ACA were then prepared similarly to a previous work.[4] Briefly, 220 μL of the NPL stock solution was added to a vial containing 300 μL of a chlorobenzene solution containing various amounts of ACA. These concentrations were optimized from the resultant UC QY upon the addition of DPA.

UC Solution Preparation

UC solutions were prepared by adding 200 μL of the NPL/ACA solution to 150 μL of a 10 mg/mL DPA solution in chlorobenzene. These solutions were prepared in a glovebox with an N_2 atmosphere to avoid oxygen exposure.

Visible Absorption Spectroscopy

Visible absorption spectra were measured using a Thermo Scientific Evolution 220 spectrophotometer scanning from 800 to 200 nm.

Steady-State PL Emission Spectroscopy

Steady-state PL emission spectra were monitored in a homebuilt optical setup, where the emission was collected at an Ocean Optics spectrometer (HR2000+ES) under either 405 nm continuous wave (CW) (LDH-D-C-405, PicoQuant) or 532 nm pseudo-CW, 80 mHz (LDH-P-FA-530L, PicoQuant) excitation. Under 532 nm excitation, a 533 nm notch filter was used to remove laser scatter, while a 425 nm long pass filter was used for the same purpose under 405 nm excitation. All spectra were collected under 23 W/cm^2 532 nm excitation and 74 W/cm^2 405 nm excitation.

Time-Resolved PL Emission Spectroscopy

The NPL time-resolved PL emission dynamics were measured under 532 nm excitation (LDH-P-FA-530L, PicoQuant) at 1 MHz and 7.8 mW/cm^2 using 533 nm notch and 550 nm long pass filters to remove excess laser scatter. Specifically, the emission dynamics were measured using a home built time-correlated single photon counting (TCSPC) setup detailed previously,[4,5] where emission was collected at a single photon counting avalanche photodiode (Micro Photon Devices) and histogrammed by a Multiharp 150 TCSPC unit. (Picoquant).

The UC PL dynamics at longer timescales were measured using an Edinburgh LP980 flash photolysis spectrometer. UC samples were excited at 532 nm at 6.7 mW/cm^2 using a Continuum Surelite EX Nd:YAG laser in combination with a Continuum Horizon optical parametric oscillator (OPO) operated at 5 Hz. The sample emission was collected by a photomultiplier tube detector (Hamamatsu R928). A 500 nm short pass filter was used to remove excess laser scatter and NPL native emission.

UC PL Power Threshold Measurements

The power dependent nature of the UC PL emission was monitored using the TCSPC set up detailed in the previous section. The samples were excited using 532 nm excitation (LDH-P-FA-530L, PicoQuant) at 80 MHz, under varying excitation powers. The sample emission was collected through the same single photon counting avalanche photodiode, after passing through a 500 nm short pass filter and 533 nm notch filter to remove excess laser scatter and native NPL emission. The sample emission was integrated for 20 seconds. The raw source power (in mW/cm^2) was converted to an excitation density, $I_{excitations}$, using the method described in Zhou *et al*., shown in eq. 5,[6]

$$I_{excitations} = \left(\frac{I_{mW}}{1000}\right)\left(\frac{\%A}{E_J}\right) \quad (5)$$

Where I_{mW} is the raw source power, $\%A$ is the sample absorptance at the excitation wavelength, and E_J is the energy of the excitation wavelength in J.

Transmission Electron Microscopy

TEM micrographs were measured by using a JEOL-JEM ARM200cF microscope.

Nuclear Magnetic Resonance (NMR) Spectroscopy

CdSe NPLs were prepared in the manner specified in the "5.5 ML CdSe NPL Synthesis" section, except the NPLs were dispersed in toluene-d8. The ^{1}H NMR spectrum of the CdSe NPL solutions with and without ethanol were recorded on a Bruker Avance III spectrometer operating at ^{1}H frequency of 600.13 MHz with a 5 mm BBO PFG probe.

In short, the oleic acid resonances were observed, as detailed previously by Hens and coworkers.[7] The specific assignments are given in the inset in Figure 12a. When oleic acid binds, the given resonance shifts downfield and broadens. Thus, we use the integration ratio of resonance 4 free (4_f) and resonance 4 bound (4_b) to approximately quantify the fraction of bound/unbound oleic acid, as shown in Figure S12c and d.

NPL Lateral Size Determination

Using a collection of TEM micrographs (Figure 1), the length and width were obtained from individual nanoplatelets (NPLs). The length and width can either be multiplied or divided to obtain the lateral size or the aspect ratio. We define the lateral size of the NPL as the lateral size of the face facing outward on the micrograph. Table S1 and S2 yield the respective statistical breakdown of both the lateral size and the aspect ratio of each NPL size population to create the box plots shown in Figure 2 and S2, respectively.

NPL Maximum Absorption Coefficient Determination

Upon determination of the lateral size from TEM micrographs, eq. 1, originally formulated in Yeltik *et al*. and reproduced below, was used to calculate the maximum absorption coefficient, ε.[3]

$$\varepsilon = 10377045 \pm 3775479 + 1757 \pm 21(LS)^{1.60} \quad (1)$$

Here, the LS corresponds to the lateral size in nm^2. As 'maximum' suggests, all terms were added together to yield ε in units of L mol^{-1} cm^{-1}, tabulated for each size in Table S3.

Stern-Volmer Quenching Analysis

Stern-Volmer quenching analysis was employed to quantitatively determine the degree of quenching according to the Stern-Volmer equation shown in eq. 2.

$$\frac{\tau_0}{\tau} = \mathrm{K}_{SV}[Q] + 1 \quad (2)$$

Here, $\frac{\tau_0}{\tau}$ is the ratio of the native lifetime of the NPL and the lifetime in the presence of a quencher, Q, ACA in this case, and K_{SV} is the Stern-Volmer quenching constant. Further, the bimolecular quenching constant, k_q, can be obtained, provided the native NPL lifetime is known, according to eq. 3.

$$\mathrm{K}_{SV} = k_q \tau_0 \quad (3)$$

As NPL lifetimes are complex and multiexponential in nature,[8] we defined τ as the time at which the PL decayed to 1/e intensity. The K_{SV} was obtained by first extracting τ for each NPL population for all ACA concentrations, shown in Figure S4. The $\frac{\tau_0}{\tau}$ ratio, subtracted by 1, was plotted against the ACA concentration, in the fashion of eq. 2. The data was fit with a linear least squares model, with the intercept fixed at 0. The obtained constants and Stern-Volmer plots are shown in Figure S5.

Determination of ACA Ligand Concentration

The ligand surface concentration was determined after first mixing the 'optimal' NPL/ACA solutions (optimized to the UC QY) as described above. An equivalent volume of ethanol was added, followed by centrifugation at 6000 rpm for 10 min. The "crashed" NPL/ACA solution was then redispersed in a 11:15 mixture of hexane and chlorobenzene, as they were before they were crashed out of solution. The concentration of both the NPL and ACA were determined using absorption spectroscopy calculated using eq. 4,

$$A = \varepsilon b C \quad (4)$$

Where A is the absorbance at a given wavelength, ε is the absorption coefficient in M^{-1} cm^{-1}, b is the pathlength in cm, and C is the concentration. For ACA, the absorption coefficient was 7800 M^{-1} cm^{-1} at 389 nm, given by Rigsby *et al.*[9]

The ratio of the concentration of ACA/NPL was termed *n and* is shown in Table S5 for all size distributions. The surface concentration, σ, was determined by dividing the ratio, n, by the area of the nanoplatelet, A_{NPL}, given in eq. 5.[7]

$$A_{NPL} = 2lw + 2wh + 2lh \quad (5)$$

Here, *l*, *w*, and *h*, correspond to the length, width, and thickness of the NPL, respectively. σ, in cm^2, is given for each NPL size in Table S5. It should be noted that this approach yields the ACA concentration of the 'crashed' solution, and may vary from the other NPL/ACA and NPL/ACA/DPA solutions described in the main text, as ethanol addition can induce stacking and surface defects,[10] and the ligand binding environment has previously shown to be dynamic.[7]

Upconversion Quantum Yield Calculations

The UC QY was calculated using eq. 6.

$$UC\ QY = \Phi_{std}\left(\frac{A_{std}}{A_{UC}}\right)\left(\frac{I_{UC}}{I_{std}}\right)\left(\frac{\eta_{UC}}{\eta_{std}}\right)^2 \quad (6)$$

Where Φ_{std} corresponds to the PL QY of a standard, rubrene in this case, $\left(\frac{A_{std}}{A_{UC}}\right)$ and $\left(\frac{I_{UC}}{I_{std}}\right)$ correspond to the ratios of the absorbance of the standard and UC solutions at 532 nm, and the integrated emission, respectively, and $\left(\frac{\eta_{UC}}{\eta_{std}}\right)^2$ refers to the ratio of the refractive indices, squared. The PL QY of the rubrene standard was measured using a Hamamatsu C11347 Quantaurus QY spectrometer. In order to account for spectral losses from the 533 nm notch filter, the spectra of DPA, ACA, or rubrene taken under 405 nm excitation, were overlaid and scaled before integration, similarly to previous works.[4,5]

UC PL Fitting Dynamics

The UC PL dynamics were fit using an exponential decay equation, shown in eq. 7 (monoexponential fit) and in eq. 8 (biexponential fit).

$$I(t) = A_1\left(-\frac{t}{\tau_1}\right) \quad (7)$$

$$I(t) = A_1\left(-\frac{t}{\tau_1}\right) + A_2(-\frac{t}{\tau_2}) \quad (8)$$

Here, *I(t)* corresponds to the UC PL intensity over time, while *A* and τ correspond to the amplitude and decay lifetime of each respective component. The fit parameters shown in Figure 4 and S8 are tabulated in Tables S6 and S7.

Table S1: NPL lateral size statistical data collected using lengths and widths of individual NPLs, taken from TEM micrographs. The respective lengths and widths were multiplied together to yield lateral sizes. This statistical information was used to assemble the box plot in Figure 2a in the main text.

NPL Size Population:	NPL5	NPL10	NPL15	NPL20	NPL25
N:	326	404	344	377	374
Mean Lat. Size (nm^2):	107.3	168.7	206.0	258.4	269.6
Standard Deviation:	36.6	51.5	59.7	65.1	73.7
Minimum:	35.2	61.3	71.4	121.0	108.7
Quartile 1:	79.9	132.9	164.5	216.2	217.1
Median	105.5	162.8	194.5	250.5	259.8
Quartile 3:	130.9	200.2	242.3	296.1	311.6
Maximum:	237.2	368.8	500.5	526.9	563.6

Table S2: Statistical breakdown of NPL aspect ratios, analogous to the lateral size data in Table S1. Here, the same lengths and widths were used, but the length was divided by the width, yielding the aspect ratio. This statistical information was used to assemble the box plot in Figure S1.

NPL Size Population:	NPL5	NPL10	NPL15	NPL20	NPL25
N:	326	404	344	377	374
Mean Aspect Ratio:	4.15	4.72	4.77	4.86	4.58
Standard Deviation:	1.25	1.30	1.28	1.15	1.13
Minimum:	1.21	1.98	2.12	1.83	1.63
Quartile 1:	3.31	3.86	4.01	4.09	3.81
Median:	3.91	4.55	4.63	4.72	4.46
Quartile 3:	4.68	5.37	5.33	5.48	5.21
Maximum:	10.57	14.31	14.04	9.81	8.74

Table S3: Absorption coefficient calculated from eq. 1 for each NPL size.

NPL Size Population:	NPL5	NPL10	NPL15	NPL20	NPL25
Maximum Absorption Coefficient ($L\ mol^{-1}\ cm^{-1}$)	1.419×10^7	1.423×10^7	1.426×10^7	1.431×10^7	1.432×10^7

Table S4: UC QY for each NPL/ACA sample of varying NPL size and ACA concentration. The UC QYs were calculated using eq. 2.

[ACA] (mM):	UC QY (%):
NPL5	
0.07	3.16
0.14	3.49
0.21	3.53
0.28	4.60
0.36	4.44
NPL10	
0.07	1.45
0.14	1.52
0.21	1.91
0.28	2.29
0.36	2.35
NPL15	
0.07	1.39
0.14	1.40
0.21	1.42
0.28	2.19
0.36	1.96
NPL20	
0.07	0.63
0.14	0.69
0.21	0.76
0.28	1.16
0.36	1.09
NPL25	
0.07	0.75
0.14	0.82
0.21	0.86
0.28	0.90
0.36	0.77

Table S5: UC figures of merit for each NPL size distribution, including the maximum UC QY for each NPL/ACA/DPA system, and the power threshold, I_{th} given in both raw source intensity (mW cm^{-2}) and converted to an excitation density (excitations s^{-1} cm^{-2}).

NPL Size Population:	Maximum UC QY (%)	I_{th} (excitations s^{-1} cm^{-2})	I_{th} (mW cm^{-2})
NPL5/ACA/DPA	4.60	4.07×10^{17}	57.2
NPL10/ACA/DPA	2.35	1.74×10^{17}	20.9
NPL15/ACA/DPA	2.19	6.04×10^{16}	6.70
NPL20/ACA/DPA	1.16	4.94×10^{16}	5.26
NPL25/ACA/DPA	0.90	3.20×10^{16}	3.18

Table S6: The calculated [ACA]/[NPL] ratio, *n*, ligand surface concentration, σ, and NPL area.

NPL Size Population:	*n*:	σ (nm^{-2}):	NPL Area (nm^{-2})
NPL5	1280	3.99	321
NPL10	1313	2.75	478
NPL15	1453	2.56	568
NPL20	1335	1.92	695
NPL25	1254	1.75	717

Table S5: Exponential decay fitting parameters for the UC PL dynamics shown in Figure S8 for all 5 size populations, and in Figure S9 for the NPL/ACA UC dynamics.

	A_1	τ_1 (μs)	A_2	τ_2 (μs)
NPL5	0.716	20.8	0.284	754
NPL10	1	14.6		
NPL15	1	16.4		
NPL20	1	11.2		
NPL25	1	12.7		
NPL/ACA	1	1410		

Table S6: Exponential decay fitting parameters for the time-resolved UC PL decays shown in Figure 4a, for two NPL sensitizer sizes, NPL5 and NPL25 with and without 20 μL of ethanol added.

	A_1	τ_1 (μs)	A_2	τ_2 (μs)
NPL5	0.722	20.9	0.278	753
NPL5/EtOH	0.943	9.8	0.0566	594
NPL25	1	16.0		
NPL5/EtOH	1	10.5		

SI Figures:

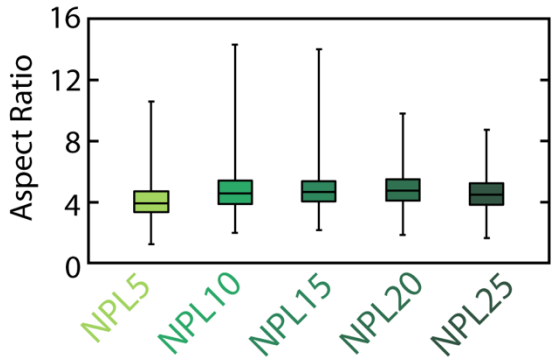

Figure S1: Box plot of the aspect ratio of each NPL size, calculated from lengths and widths of individual NPLs from TEM micrographs.

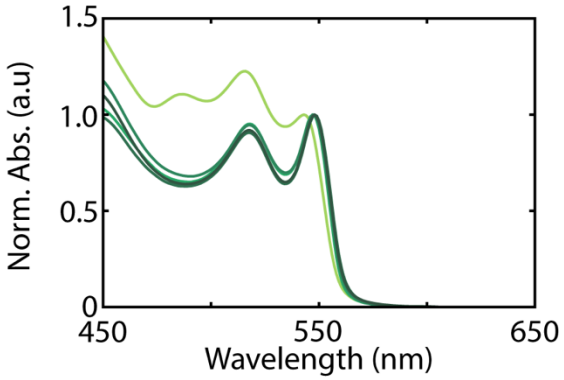

Figure S2: Normalized absorption spectrum of each NPL size, where each trace is normalized to 1 at its first excitonic absorption feature. The NPL5 (light green) trace is slightly blue shifted due to additional quantum confinement.

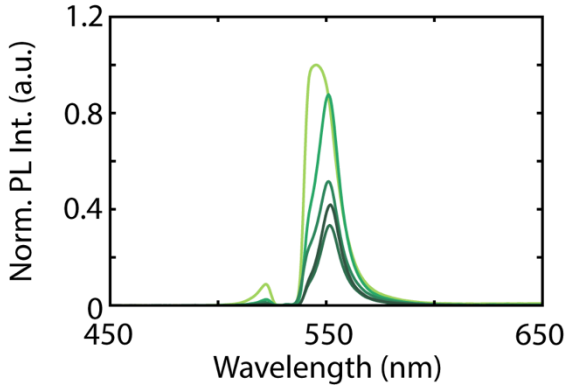

Figure S3: NPL PL emission spectra of the native NPL samples excited at 532 nm and normalized by the NPL PL QY, analogous to Figure 2c. A 533 nm notch filter was used to remove the laser excitation, which also removed some NPL emission.

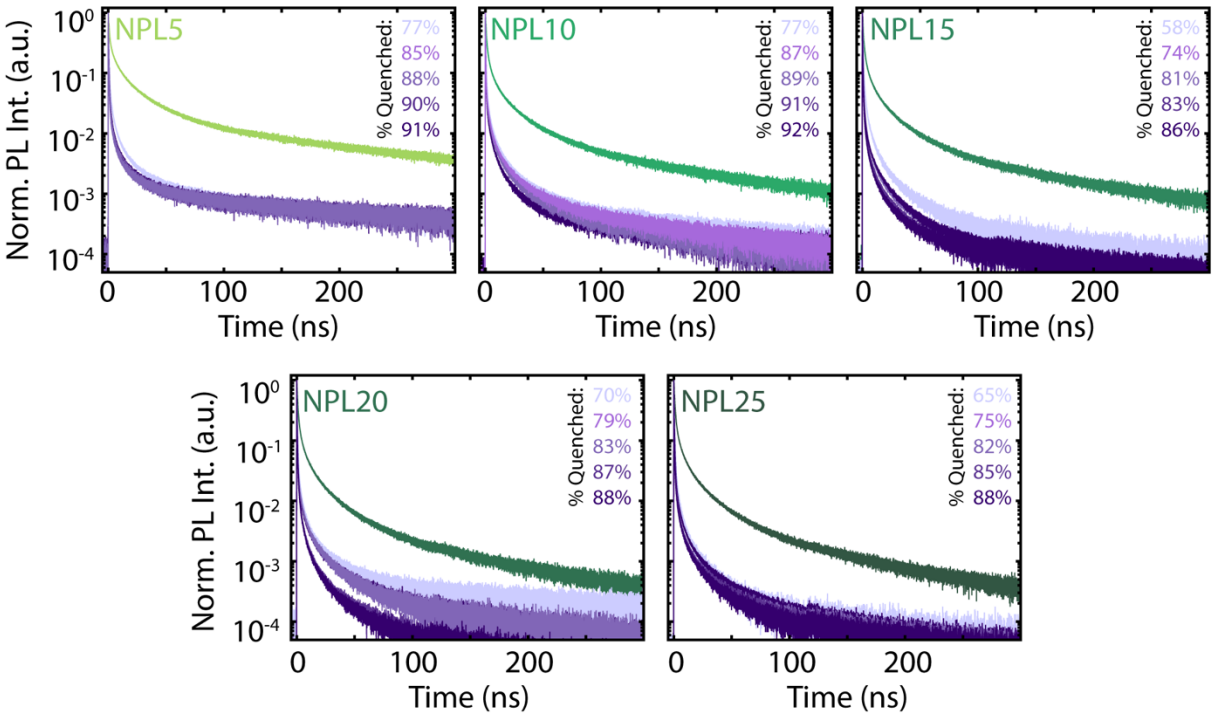

Figure S4: NPL/ACA time-resolved emission quenching for each NPL size. The NPL PL emission was measured using 532 nm excitation at 1 MHz. A 533 nm notch filter and 550 nm long pass filter were used to remove excess laser scatter. The degree of quenching was calculated using eq. 1 in the main text.

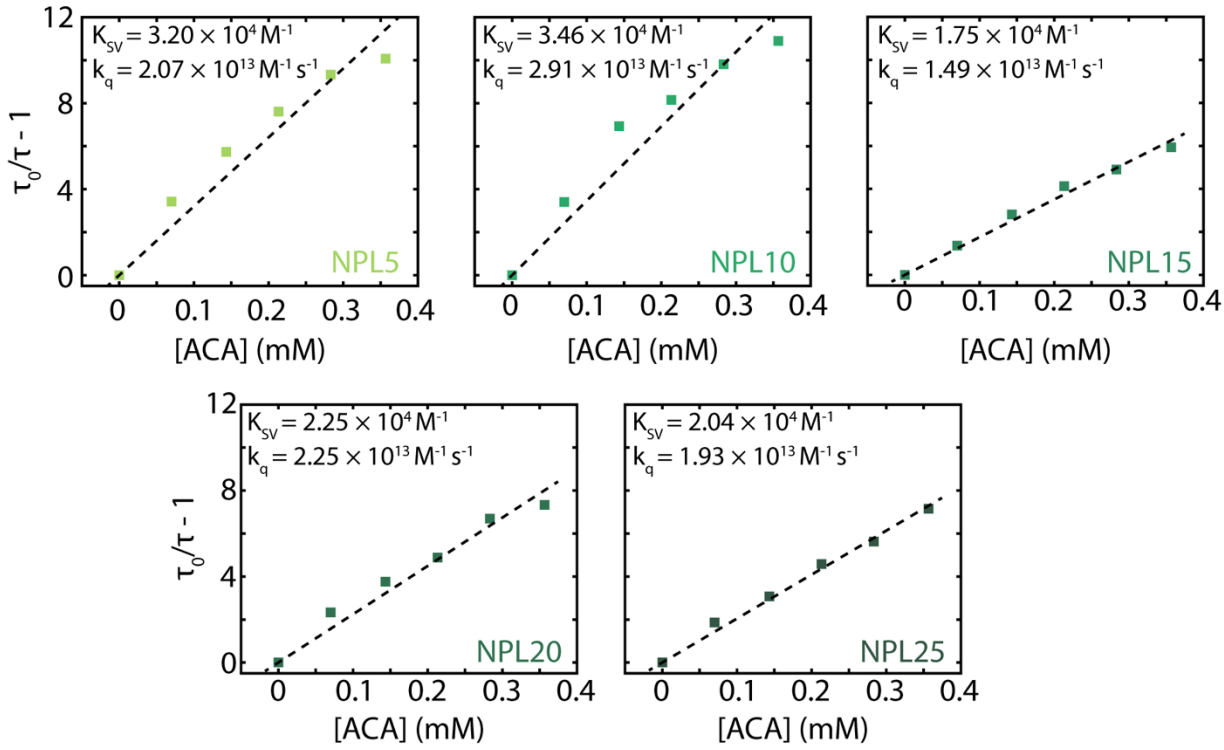

Figure S5: Stern-Volmer plot detailing the degree of quenching of native NPL time-resolved emission upon the addition of ACA transmitter ligand. The Stern-Volmer constant, K_{SV}, and bimolecular quenching constant, k_q, are obtained via the linear fit of the data (see section titled Stern-Volmer Analysis for more detail).

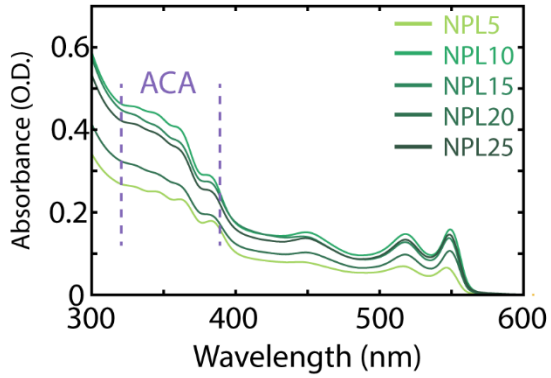

Figure S6: Absorbance spectrum of the crashed NPL/ACA solutions used to determine the ligand surface concentration found in Table S5.

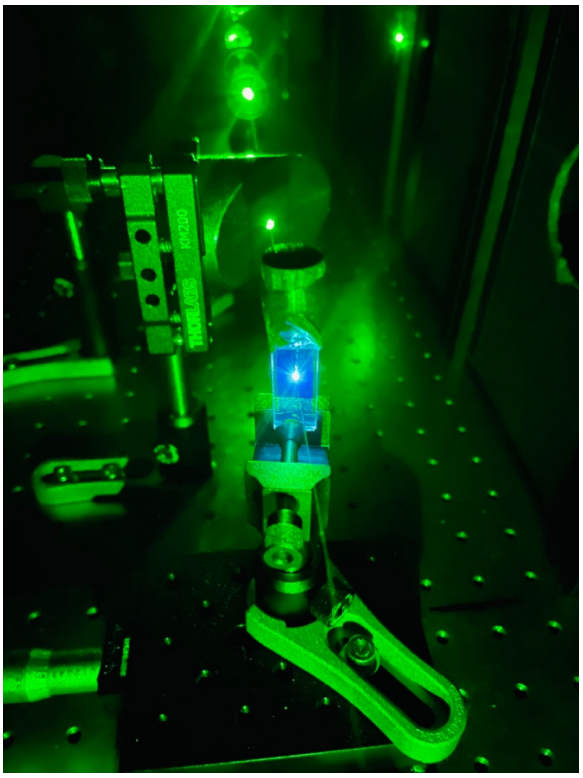

Figure S7:Photograph of the upconverted emission from the champion NPL5/ACA/DPA sample under 532 nm excitation.

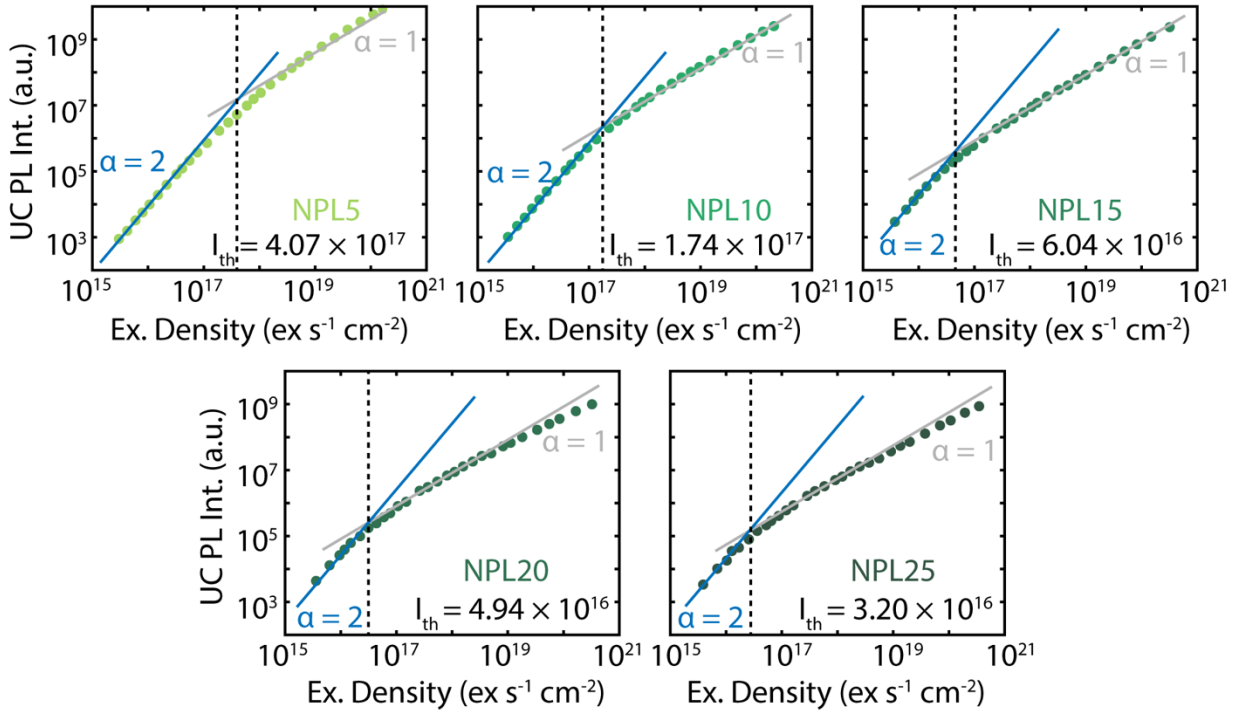

Figure S8: Log-log plot of the UC PL intensity vs. the excitation density for TTA-UC systems sensitized by each NPL size, converted from the raw excitation density from a 532 nm laser operating under pseudo-continuous wave (80 mHz). A slope α = 2 to slope α = 1 change occurs at the power threshold, I_{th}, characteristic of TTA-UC systems. The plots are ordered from NPL5 (top left) to NPL25 (bottom right).

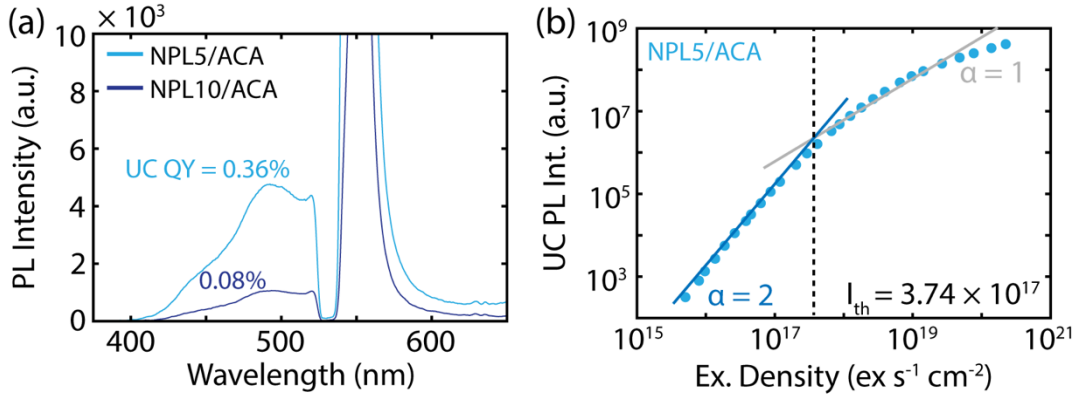

Figure S9: Steady-state PL emission spectra of the UC emission from ACA in NPL5/ACA (light blue) and NPL10/ACA (dark blue) solutions. (b) UC PL power dependence plot of the NPL5/ACA solution, yielding the I_{th} at the point where the two slope regimes meet. The solutions were excited using pseudo continuous wave 532 nm emission (80 mHz), and a 533 nm notch filter was used to remove excess laser scatter in (a) and a 500 nm short pass filter in (b).

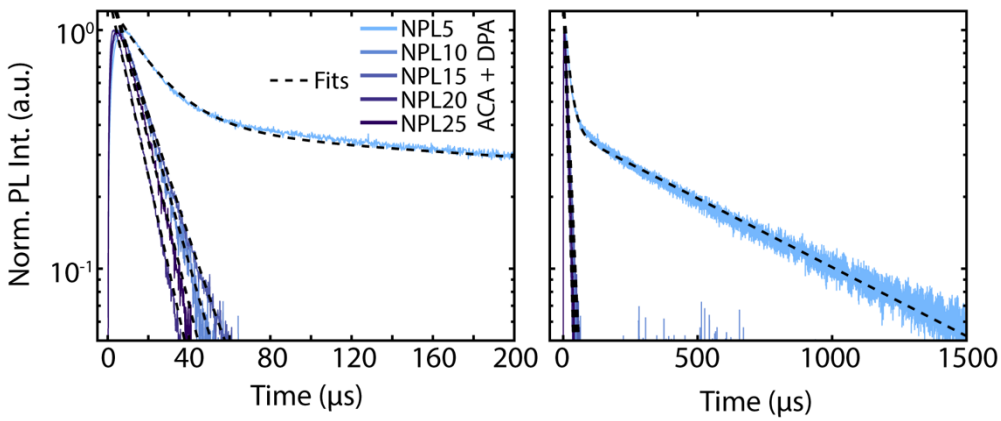

Figure S10: Time resolved PL emission dynamics of the UC PL from NPL/ACA/DPA solutions using NPLs of various lateral sizes to 200 µs (left) and to 1.5 ms (right). The UC time resolved emission was measured under 532 nm excitation, where the excess laser scatter and native NPL emission was removed by a 500 nm short pass filter. The exponential fitting functions are tabulated in Table S7.

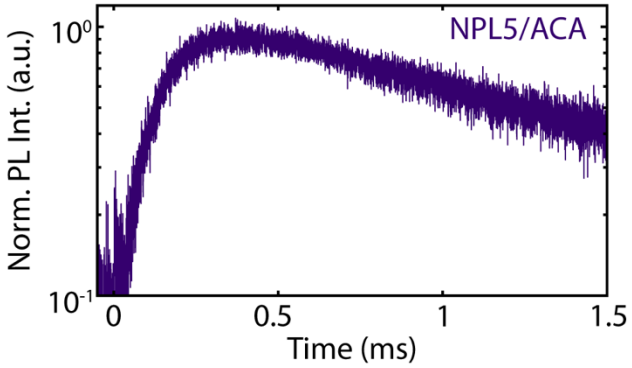

Figure S11: Time resolved PL emission dynamics of the UC PL from the NPL5/ACA sample. The UC time resolved emission was measured under 532 nm excitation, where the excess laser scatter and native NPL emission was removed by a 500 nm short pass filter.

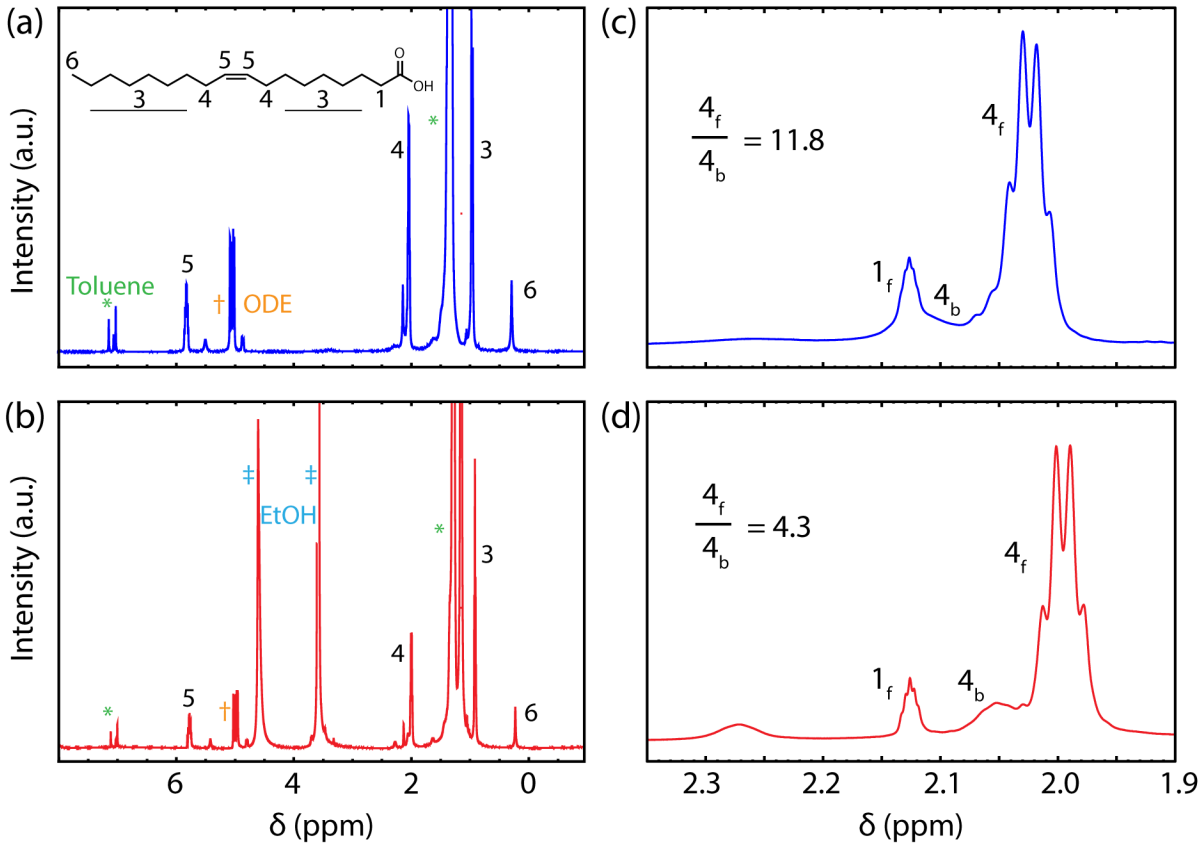

Figure S12: [1]H NMR spectra of a representative CdSe nanoplatelet (a) before and (b) after the addition of ethanol. The assignments of the oleic acid ligand are shown in the inset in (a), while additional peaks due to residual solvent are labeled in their respective spectra. A zoom in of the spectra are shown in (c) and (d) of (a) and (b), respectively, showing resonance 4 and the relevant integration ratio of the bound (4_b) and unbound (4_f) resonances.

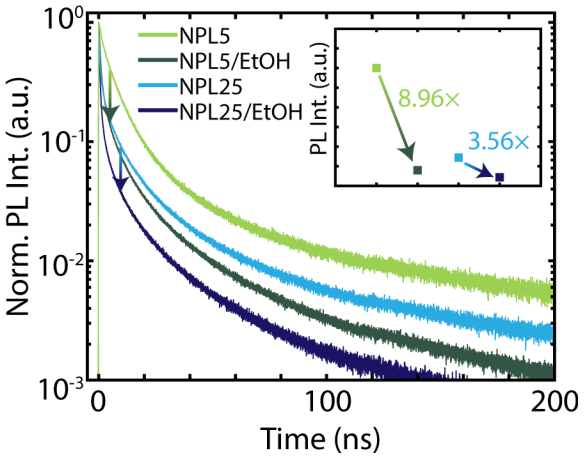

Figure S13: Time resolved PL emission dynamics of the NPL5 and NPL25 stock solutions before (light green and light blue, respectively), and after ethanol addition (dark green and dark blue). The concomitant decrease in PL intensity upon ethanol addition is shown in the inset.

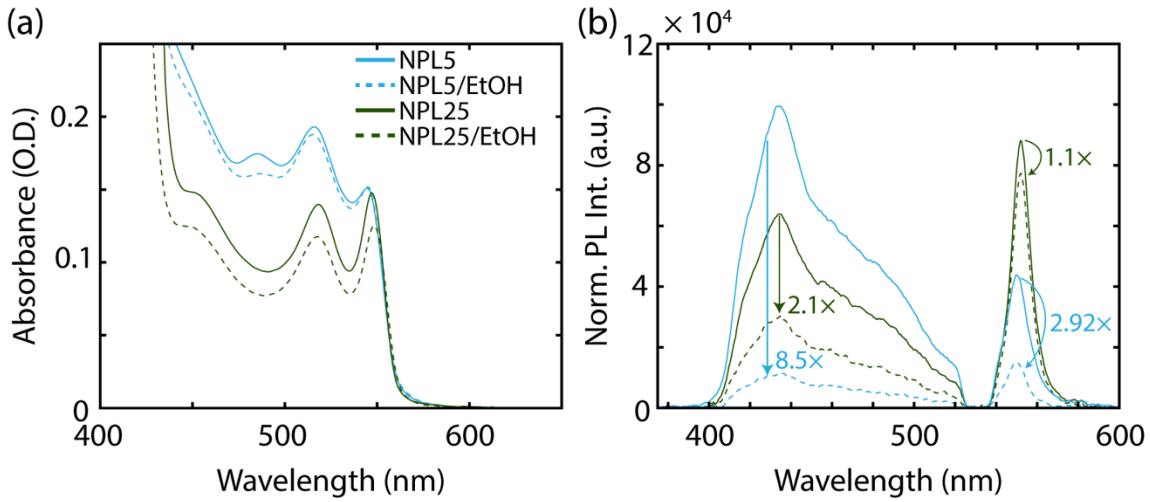

Figure S14: (a) Absorption spectrum of native NPL5 and NPL25 and NPL5 and NPL25 with 20 µL of ethanol added. (b) UC emission spectra of NPL5 and NPL25 with and without 20 µL of ethanol added. The UC emission was normalized by the excitonic absorption peak shown in (a). The addition of ethanol results in a decrease in the UC PL intensity and the NPL PL intensity to different degrees, as shown by the corresponding arrows.

REFERENCES

(1) Bertrand, G. H. V.; Polovitsyn, A.; Christodoulou, S.; Khan, A. H.; Moreels, I. Shape Control of Zincblende CdSe Nanoplatelets. *Chem. Commun.* **2016**, *52* (80), 11975–11978. https://doi.org/10.1039/C6CC05705E.

(2) Ithurria, S.; Tessier, M. D.; Mahler, B.; Lobo, R.; Dubertret, B.; Efros, A. L. Colloidal Nanoplatelets with Two-Dimensional Electronic Structure. *Nat. Mater.* **2011**, *10* (12), 936–941. https://doi.org/10.1038/nmat3145.

(3) Yeltik, A.; Delikanli, S.; Olutas, M.; Kelestemur, Y.; Guzelturk, B.; Demir, H. V. Experimental Determination of the Absorption Cross-Section and Molar Extinction Coefficient of Colloidal CdSe Nanoplatelets. *J. Phys. Chem. C* **2015**, *119* (47), 26768–26775. https://doi.org/10.1021/acs.jpcc.5b09275.

(4) VanOrman, Z. A.; Bieber, A. S.; Wieghold, S.; Nienhaus, L. Green-to-Blue Triplet Fusion Upconversion Sensitized by Anisotropic CdSe Nanoplatelets. *Chem. Mater.* **2020**, *32* (11), 4734–4742. https://doi.org/10.1021/acs.chemmater.0c01354.

(5) VanOrman, Z. A.; Conti, C. R.; Strouse, G. F.; Nienhaus, L. Red-to-Blue Photon Upconversion Enabled by One-Dimensional CdTe Nanorods. *Chem. Mater.* **2021**, *33* (1), 452–458. https://doi.org/10.1021/acs.chemmater.0c04468.

(6) Zhou, Y.; Ruchlin, C.; Robb, A. J.; Hanson, K. Singlet Sensitization-Enhanced Upconversion Solar Cells via Self-Assembled Trilayers. *ACS Energy Lett.* **2019**, *4* (6), 1458–1463. https://doi.org/10.1021/acsenergylett.9b00870.

(7) Singh, S.; Tomar, R.; ten Brinck, S.; De Roo, J.; Geiregat, P.; Martins, J. C.; Infante, I.; Hens, Z. Colloidal CdSe Nanoplatelets, A Model for Surface Chemistry/Optoelectronic Property Relations in Semiconductor Nanocrystals. *J. Am. Chem. Soc.* **2018**, *140* (41), 13292–13300. https://doi.org/10.1021/jacs.8b07566.

(8) Naeem, A.; Masia, F.; Christodoulou, S.; Moreels, I.; Borri, P.; Langbein, W. Giant Exciton Oscillator Strength and Radiatively Limited Dephasing in Two-Dimensional Platelets. *Phys. Rev. B* **2015**, *91* (12), 121302. https://doi.org/10.1103/PhysRevB.91.121302.

(9) Rigsby, E. M.; Miyashita, T.; Jaimes, P.; Fishman, D. A.; Tang, M. L. On the Size-Dependence of CdSe Nanocrystals for Photon Upconversion with Anthracene. *J. Chem. Phys.* **2020**, *153* (11), 114702. https://doi.org/10.1063/5.0017585.

(10) Guzelturk, B.; Erdem, O.; Olutas, M.; Kelestemur, Y.; Demir, H. V. Stacking in Colloidal Nanoplatelets: Tuning Excitonic Properties. *ACS Nano* **2014**, *8* (12), 12524–12533. https://doi.org/10.1021/nn5053734.